

Coupling of NBI-driven CAEs to Kinetic Alfvén Waves in NSTX and energy channelling

Elena Belova

In collaboration with: N. N. Gorelenkov, N. A. Crocker,
E. D. Fredrickson, K. Tritz

NSTX Meeting January 2014

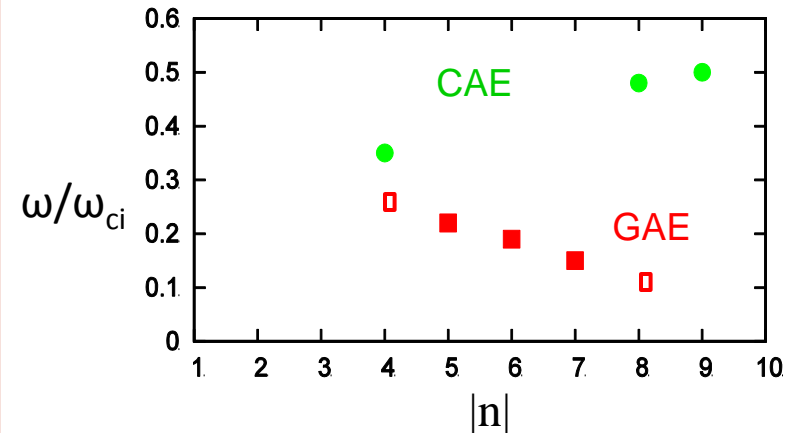
GAE and CAE modes observed in NSTX shot # 141398

Experimental measurements

[N. Crocker, IAEA 2012, EX/P6-02]

- Detailed measurements of GAE and CAE modes amplitudes and mode structure were obtained for H-mode plasma in NSTX shot 141398.
- The modes have been identified as CAE modes for frequencies $f > 600$ kHz, and small toroidal mode numbers $|n| \leq 5$.
- The modes have been identified as GAEs for $f < 600$ kHz, and $|n| \sim 6-8$ based on dispersion relations.

HYM simulations



Frequency versus toroidal mode number for most unstable GAE (red) and CAE (green) modes, from HYM simulations for NSTX shot #141398. Frequency is normalized to ion cyclotron frequency at the axis $f_{ci}=2.5$ MHz.

HYM simulations show that most unstable modes for $n=5-7$ are **counter-rotating GAE modes**, with shear Alfvén wave polarization in the core and $f=380-550$ kHz. The $n=4$ and $n=8$ and $n=9$ modes are **co-rotating CAE modes** with $f=870-1200$ kHz, which have been identified based on large compressional component of perturbed magnetic field.

Self-consistent MHD + fast ions coupling scheme

Background plasma - fluid:

$$\rho \frac{d\mathbf{V}}{dt} = -\nabla p + (\mathbf{j} - \mathbf{j}_i) \times \mathbf{B} - n_i (\mathbf{E} - \eta \mathbf{j})$$

$$\mathbf{E} = -\mathbf{V} \times \mathbf{B} + \eta \mathbf{j}$$

$$\mathbf{B} = \mathbf{B}_0 + \nabla \times \mathbf{A}$$

$$\partial \mathbf{A} / \partial t = -\mathbf{E}$$

$$\mathbf{j} = \nabla \times \mathbf{B}$$

$$\partial p^{1/\gamma} / \partial t = -\nabla \cdot (\mathbf{V} p^{1/\gamma})$$

$$\partial \rho / \partial t = -\nabla \cdot (\mathbf{V} \rho)$$

Fast ions – delta-F scheme:

$$\frac{d\mathbf{x}}{dt} = \mathbf{v}$$

$$\frac{d\mathbf{v}}{dt} = \mathbf{E} - \eta \mathbf{j} + \mathbf{v} \times \mathbf{B}$$

$w = \delta F / F$ - particle weight

$$\frac{dw}{dt} = -(1-w) \frac{d(\ln F_0)}{dt}$$

$$F_0 = F_0(\varepsilon, \mu, p_\phi)$$

ρ , \mathbf{V} and p are bulk plasma density, velocity and pressure, n_i and \mathbf{j}_i are fast ion density and current, $n_i \ll n$ – is assumed.

Equilibrium calculations

Equilibrium distribution function $F_0 = F_1(v)F_2(\lambda)F_3(p_\phi)$

$$F_1(v) = \frac{1}{v^3 + v_*^3}, \quad \text{for } v < v_0$$

$$F_2(\lambda) = \exp(-(\lambda - \lambda_0)^2 / \Delta\lambda^2)$$

$$F_3(p_\phi) = \frac{(p_\phi - p_0)^\beta}{(R_0 v - \psi_0 - p_0)^\beta}, \quad \text{for } p_\phi > p_0$$

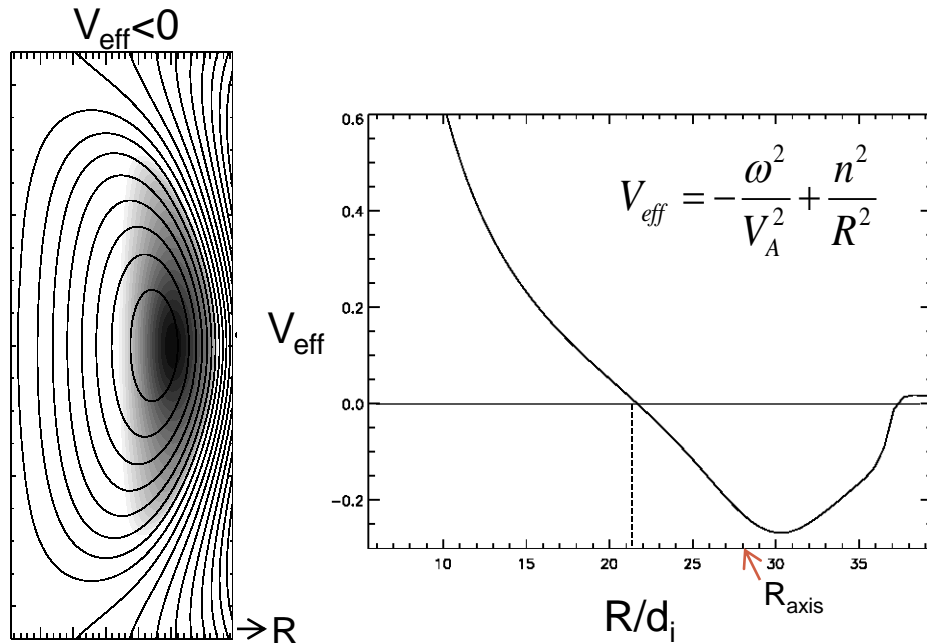
where $v_0 \approx 3v_A$, $v_* = v_0/\sqrt{3}$, $\lambda = \mu B_0/\varepsilon$ - pitch angle,
 $\lambda_0 = 0.8 - 1$,

and $\mu = \mu_0 + \mu_1$ includes first-order corrections [Littlejohn'81]:

$$\mu = \frac{(\mathbf{v}_\perp - \mathbf{v}_d)^2}{2B} - \frac{\mu_0 v_\parallel}{2B} [\hat{\mathbf{b}} \cdot \nabla \times \hat{\mathbf{b}} - 2(\hat{\mathbf{a}} \cdot \nabla \hat{\mathbf{b}}) \cdot \hat{\mathbf{c}}]$$

\mathbf{v}_d is magnetic gradient and curvature drift velocity, $\hat{\mathbf{c}} = \mathbf{v}_\perp/v_\perp$,
 $\hat{\mathbf{a}} = \hat{\mathbf{b}} \times \hat{\mathbf{c}}$

n=8 CAE mode: effective potential well



Contour plot and radial profile of the effective potential V_{eff} for n=8 CAE mode with $\omega=0.48\omega_{\text{ci0}}$. Mode can exist for $V_{\text{eff}} < 0$ with radial extent: $22 < R < 37$ (major radius is normalized to ion skin depth $d_i=3.93\text{cm}$).

Approximate equation for CAE mode, assuming circular cross-section, and neglecting beam effects and coupling to SAW:

$$\frac{\partial^2 \delta B_{\parallel}}{\partial r^2} = V_{\text{eff}} \delta B_{\parallel}$$

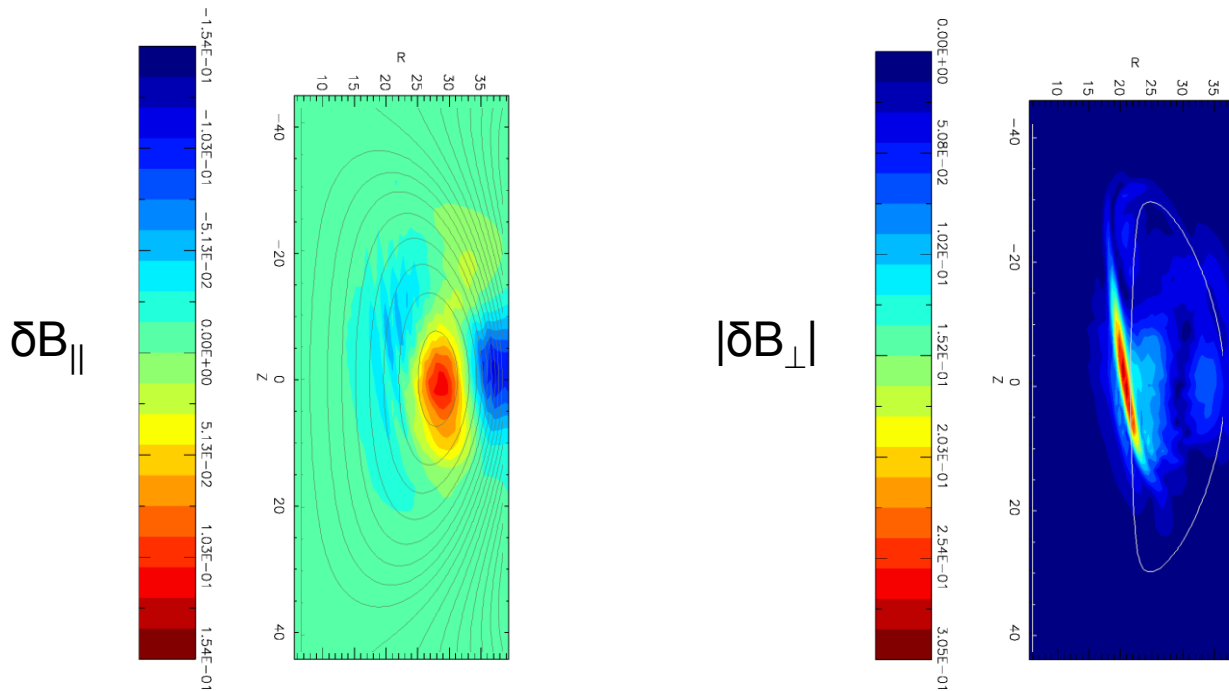
$$V_{\text{eff}} = -\frac{\omega^2}{V_A^2} + k_{\parallel}^2$$

HYM simulations show unstable n=8 mode with $\omega=0.48\omega_{\text{ci0}}$ and $\gamma=0.004\omega_{\text{ci0}}$.

Effective potential well for n=8 mode is narrower and deeper than V_{eff} for n=4 resulting in more localized CAE mode with larger frequency.

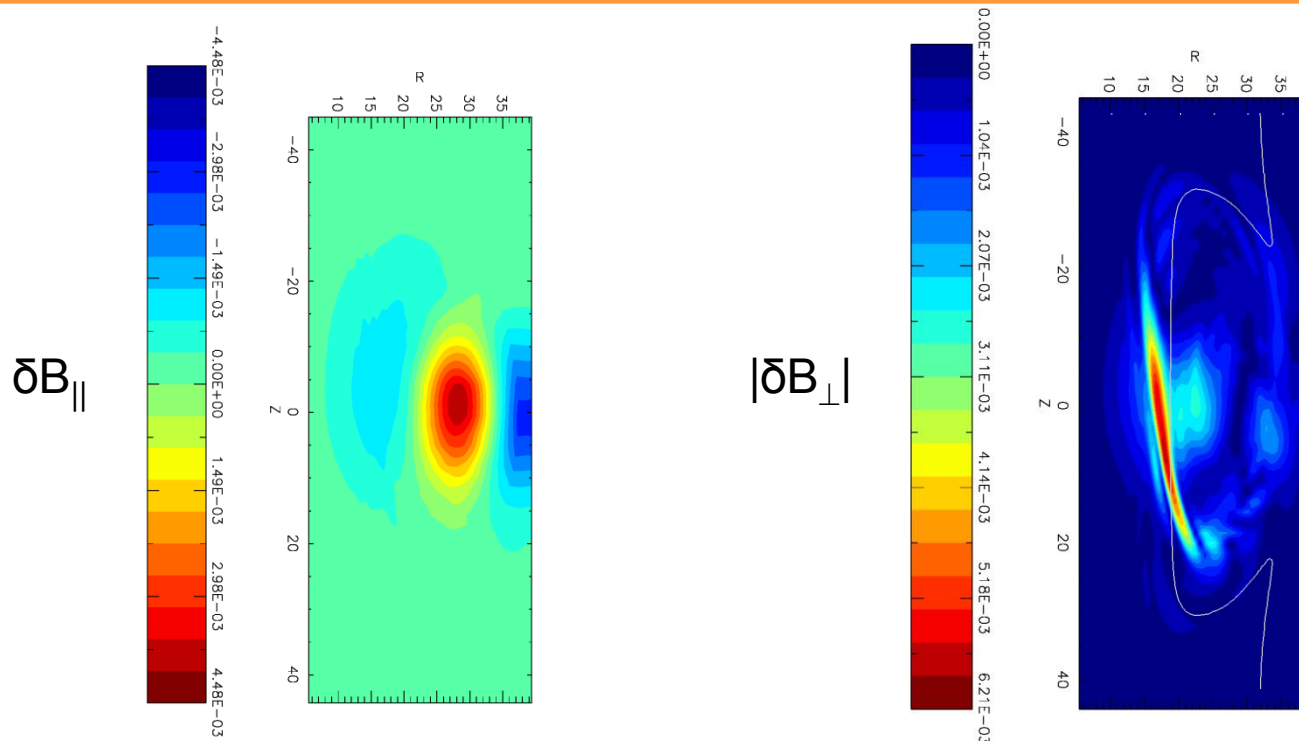
Edge of CAE well coincides with resonance location \rightarrow CAE/KAW coupling.

n=8 co-rotating CAE: mode structure



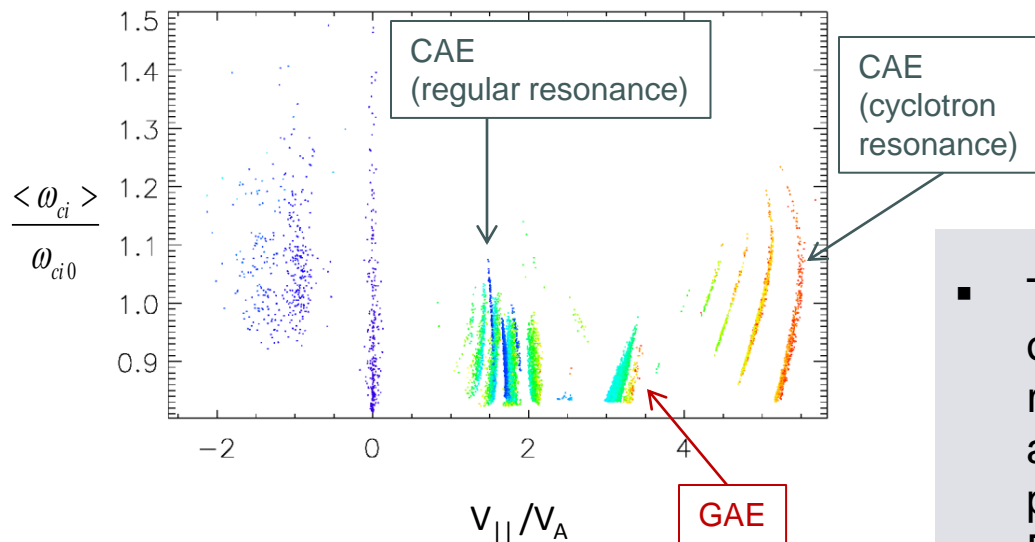
Higher- n co-rotating CAEs show resonant coupling to KAW. CAE mode peaks near magnetic axis, where $\delta B_{\parallel} \gg \delta B_{\perp}$, KAW is located at the resonance (solid contour line of $\omega_A(Z,R) = \omega_{CAE}$) on HFS.

n=4 CAE structure: compressional vs shear components



KAW structure is tilted relative to equilibrium magnetic field because k_{\parallel} is in the direction of the beam velocity, and k_{\perp} directed towards high-density side with $k_{\perp} \gg k_{\parallel}$. This results in a mode structure which is not symmetric relative to mid-plane.

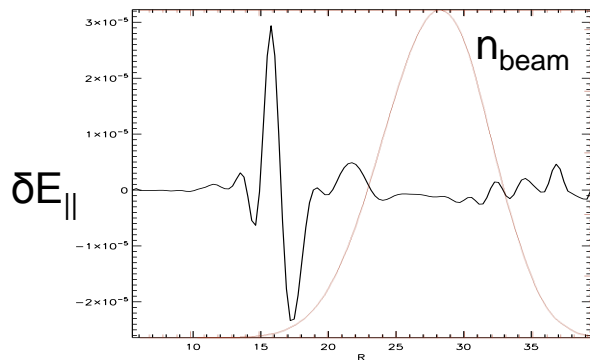
Resonant particles



Orbit-averaged cyclotron frequency vs orbit-averaged parallel velocity for resonant particles. From simulations for $n=8$ ($\omega=0.48\omega_{ci0}$, $\gamma=0.004\omega_{ci0}$). Particle color corresponds to different energies: from $E=0$ (purple) to $E=90\text{keV}$ (red).

- Two groups of resonant particles, one group which satisfies the regular resonance: $\omega - k_{||}v_{||}=0$, and a group of higher energy particles which satisfy the Doppler-shifted cyclotron resonant condition: $|\omega| + \omega_{ci} - k_{||}v_{||}=0$.
- Main contribution comes from the beam ions with $v_{||} \sim \omega/k_{||}$, and the contribution from the cyclotron resonances is negligible.

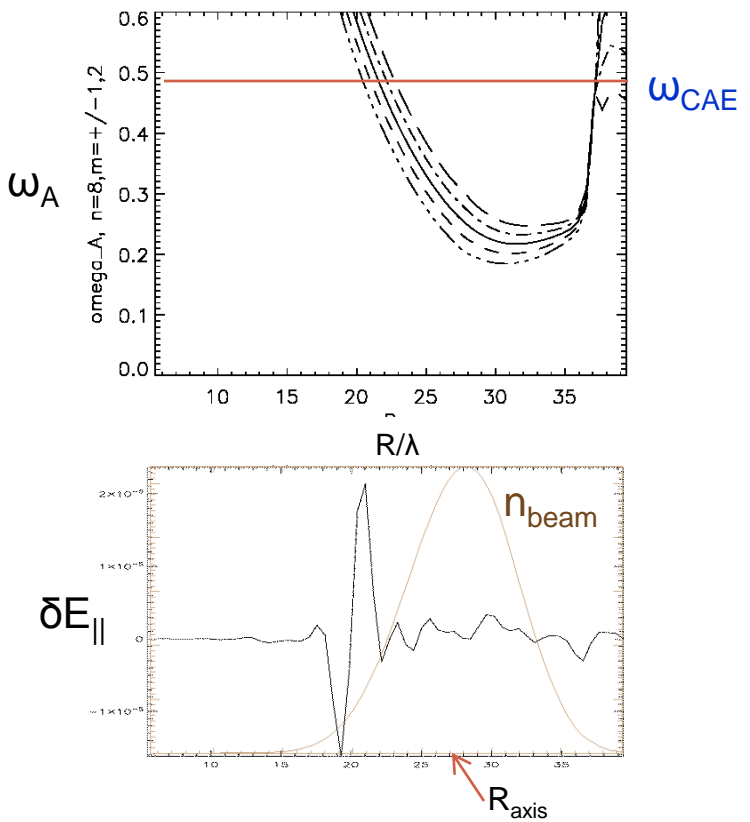
KAW structure



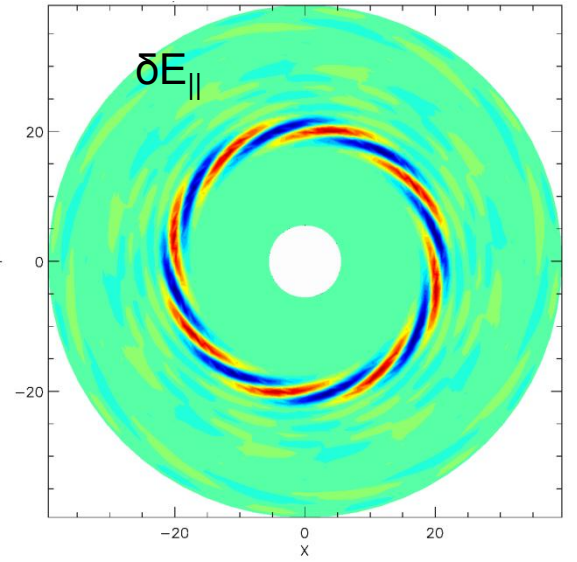
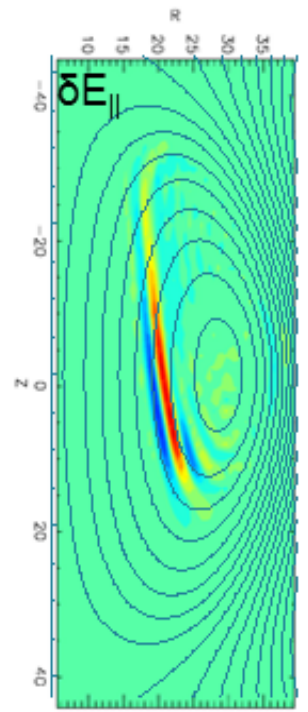
Radial profiles of δE_{\parallel} and beam ion density for n=4 CAE/KAW.

- Resonance with KAW is located at the edge of CAE well, and just inside beam ion density profile.
- Resonant mode polarization is consistent with KAW mode, ie $\delta B_z \gg \delta B_R, \delta B_{\parallel}$ and $\delta V_z \gg \delta V_R, \delta V_{\parallel}$ with $\delta V_z \sim -\delta B_z$.
- Radial width of KAW is comparable to beam ions Larmor radius, $k_{\perp} \rho_{\text{beam}} \sim 1$.

Low-n and high-n CAE modes show coupling to KAW



Radial profiles of Alfvén continuum and δE_{\parallel} for $n=8$. Radial width of KAW is comparable to beam ions Larmor radius.



Poloidal and equatorial plane contour plots of δE_{\parallel} , solid line is contour of $\omega_A(Z,R) = \omega_{CAE}$, where $\omega_A(Z,R) = V_A n/R$.

KAW can have strong effect on electron transport due to finite δE_{\parallel} .

KAW dispersion relation

- assuming three-component plasma, Maxwellian ions with $V_0=0$, and including only adiabatic beam ions response (non-perturbative).

$$\text{KAW in full kinetic model: } \omega^2 = k_{\parallel}^2 V_A^2 \left(1 + \lambda_e + \frac{3 n_i}{4 n_e} \lambda_i + \frac{3 n_b}{4 n_e} \lambda_b - \frac{\omega^2}{\omega_{ci}^2} \right),$$

$$\text{where } \lambda_{\alpha} = \frac{k_{\perp}^2 T_{\alpha}}{m_i \omega_{ci}^2}$$

$$\text{KAW in HYM model: } \omega^2 = k_{\parallel}^2 V_A^2 \left(1 + \frac{3 n_b}{4 n_e} \lambda_b - \frac{n_b}{n_e} \frac{\omega^2}{\omega_{ci}^2} \right), \quad \lambda_b = \frac{k_{\perp}^2 T_b}{m_i \omega_{ci}^2}$$

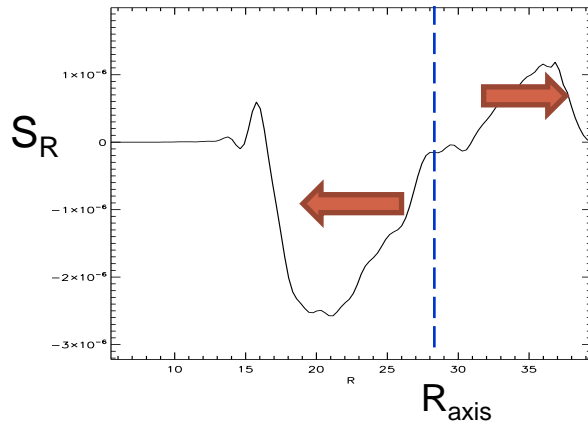
- consistent with full kinetic in the limit $\lambda_e \rightarrow 0$, $\lambda_i \rightarrow 0$, and $\omega \ll \omega_{ci}$.

Scale-length for beam-KAW is the beam ion Larmor radius.

CAE/KAW coupling also shown by TORIC ICRF code

- TORIC solves the wave equation using a fully kinetic model for the plasma dielectric response.
- An antenna-driven CAE and related KAW have been found for $n=1$, with δE_{\parallel} and CAE/KAW structures similar to those in HYM [APS2013].
- The TORIC model did not include a fast ion component, and the radial scale of the KAW was likely related to the thermal ion FLR.

Relation between CAE/KAW and T_e flattening?



Radial component of quasilinear Poynting vector $\mathbf{S} = \langle \mathbf{E} \times \mathbf{B} \rangle$.
Energy flux is directed away from magnetic axis, ie from CAE to KAW.

Fraction of NBI power transferred to CAE can be estimated as:

$$P = 2\gamma \int (\delta B)^2 / 4\pi d^3x,$$

where $\delta B/B_0 = (0.9-3.4) \times 10^{-3}$ corresponds to measured displacement $|\xi| = 0.1-0.4$ mm [N.Crocker'13] (based on HYM-calculated linear mode structure for the $n=4$ CAE).

For $\gamma/\omega_{ci} = 0.005-0.01$, $P = (0.013-0.4)$ MW,

- significant fraction of NBI energy can be transferred to several unstable CAEs of relatively large amplitudes.

Energy flux from the CAE to the KAW and dissipation at the resonance location can have a strong effect on the temperature profile.

Summary

- Unstable CAE modes couple with KAW on the HFS. Resonance with KAW is located at the edge of CAE well, and just inside beam ion density profile. Radial width of KAW is comparable to beam ion Larmor radius.
- A significant fraction of NBI energy can be transferred to several unstable CAEs: $P \sim 0.4 \text{ MW}$ for $\delta B/B_0 \sim 10^{-3}$.
- Energy flux from the CAE to KAW and dissipation at the resonant location can have direct effect on electron temperature profile.
- In addition, radially overlapping KAWs can strongly enhance plasma heat transport due to finite δE_{\parallel} and large width of resonant mode.
- Detailed comparison of the relative importance of the energy channelling and anomalous electron transport mechanisms will require fully nonlinear simulations, and will be performed in the future.